

Reversible Labeling of a Chemosensitizer Binding Domain of p-Glycoprotein with a Novel 1,4-Dihydropyridine Drug Transport Inhibitor^{†,‡}

R. Boer,[§] M. Dichtl,^{||} C. Borchers,[⊥] W. R. Ulrich,[§] J. F. Marecek,[▽] G. D. Prestwich,[▽] H. Glossmann,^{||} and J. Striessnig^{*,‡}

Institut für Biochemische Pharmakologie, Peter-Mayrstrasse 1, A-6020 Innsbruck, Austria, Byk-Gulden, Postfach 100310, D-78403 Konstanz, Germany, Department of Chemistry, State University of New York at Stony Brook, Stony Brook, NY 11794-3400, and Fakultät für Chemie, Universität Konstanz, Germany

Received August 14, 1995; Revised Manuscript Received November 9, 1995[⊗]

ABSTRACT: A photoreactive dihydropyridine (DHP), BZDC–DHP (2,6-dimethyl-4-(2-(trifluoromethyl)-phenyl)-1,4-dihydropyridine-3,5-dicarboxylic acid {2-[3-(4-benzoylphenyl)propionylamino]ethyl} ester ethyl ester), and its tritiated derivative were synthesized as novel probes for human p-glycoprotein (p-gp). (–)-[³H]BZDC–DHP specifically photolabeled p-gp in membranes of multidrug-resistant CCRF-ADR5000 cells. In reversible labeling experiments a saturable, vinblastine-sensitive and high-affinity ($K_d = 16.3$ nM, $B_{max} = 58$ pmol/mg of protein, $k_{+1} = 0.031$ nM^{−1} min^{−1}, $k_{−1} = 0.172$ min^{−1}) binding component was present in CCRF-ADR5000 membranes but absent in the sensitive parent cell line. Binding was inhibited by cytotoxics and known chemosensitizers with a p-gp characteristic pharmacological profile. For eight chemosensitizers tested, the potency for binding inhibition correlated ($r > 0.94$) with the potency for drug transport inhibition (measured using rhodamine 123 accumulation). The DHP niguldipine and a structurally related pyrimidine stereoselectively stimulated reversible (–)-[³H]BZDC–DHP binding, suggesting that more than one DHP molecule can bind to p-gp at the same time. Our data demonstrate that DHPs label multiple chemosensitizer domains on p-gp, distinct from the vinblastine interaction site. (–)-[³H]BZDC–DHP represents a valuable tool to characterize the molecular organization of chemosensitizer binding domains on p-gp by both reversible binding and photoinduced covalent modification. It provides a novel simple screening assay for p-gp active drugs.

p-Glycoprotein (p-gp)¹ is a transmembrane phosphoglycoprotein in the plasma membrane (150–170 kDa) of normal and tumor cells that functions as an energy-dependent multidrug transporter (Pastan & Gottesman, 1991). Tumor cells are able to acquire multidrug resistance toward a variety of cytotoxic agents by overexpressing p-gp. The pumping activity of p-gp leads to an increased drug efflux thereby diminishing cytoplasmic drug accumulation. In addition, inhibition of drug uptake has also been reported (Pastan & Gottesman, 1991; Safa et al., 1990; Stein et al., 1994). Agents that are not cytotoxic by themselves are able to reverse p-gp-mediated drug resistance by competing for the transport mechanism and/or drug binding (Pastan & Gottesman, 1991). These drugs, termed “chemosensitizers”, belong to different chemical classes (Ford & Hait, 1990; Pastan & Gottesman, 1991), including Ca²⁺ channel blockers, like dextniguldipine and verapamil (Friche et al., 1993; Hofmann et al., 1992; Boer et al., 1994), and hydrophobic

peptides (ciclosporin A, SDZ PSC 833) (Foxwell et al., 1989; Keller et al., 1992).

Although considerable progress has been made during the last years to elucidate the structure–function relationship of p-gp, the molecular mechanism of ATP-dependent drug transport is still poorly understood. As specific drug recognition must precede transport by p-gp, the understanding of the molecular organization of its drug receptor domains would also provide structural information about the drug-transporting pathway. [³H]Vinblastine was first shown to reversibly label a site for cytotoxic alkaloids with nanomolar (Ferry et al., 1992) to micromolar (Cornwell et al., 1986, 1987) dissociation constants. Safa et al. (1987) first employed the aryl azide Ca²⁺ channel blocker [³H]azidopine (Ferry et al., 1984) to identify a DHP acceptor site on p-gp with photoaffinity labeling. Photolabeling was inhibited by cytotoxics as well as chemosensitizers with a similar order of potency than reversible [³H]vinblastine labeling (Safa et al., 1987). Because many p-gp active drugs were found to block [³H]azidopine photolabeling (Foxwell et al., 1989; Kamiwatari et al., 1989; Hait et al., 1993; Horton et al., 1993), this assay was established as a biochemical tool to screen for chemosensitizers (Kamiwatari et al., 1989; Hyafil et al., 1993). Despite its relatively low affinity for p-gp, [³H]azidopine photolabeling was also successfully employed to study the effects of p-gp mutations on DHP binding (Safa et al., 1990; Kajiji et al., 1993; Loo & Clarke, 1993).

So far no radioligand has been described that allows the reversible high-affinity labeling of p-gp with a chemosensitizer. Such an assay would provide a more efficient drug screening assay than photolabeling. It would be useful to study the organization of the chemosensitizer binding domains on p-gp and their proposed noncompetitive interac

[†] This work was supported by grants from the Fonds zur Förderung der Wissenschaftlichen Forschung (S6602 to J.S.), the Hans and Blanca Moser Stiftung (to M.D.), and in part by NIH Grant NS29632 (to G.D.P.).

[‡] This work is part of the thesis of M.D.

* To whom correspondence should be addressed: Tel: +43 512 507 3164. FAX: +43 512 588 627. E-mail: joerg.striessnig@uibk.ac.at.

[§] Byk-Gulden.

^{||} Institut für Biochemische Pharmakologie.

[⊥] Fakultät für Chemie, Universität Konstanz, Germany.

[▽] State University of New York at Stony Brook.

[⊗] Abstract published in *Advance ACS Abstracts*, January 1, 1996.

¹ Abbreviations: BZDC, benzoyldihydrocinnamic acid; DHP, dihydropyridine; EC₅₀, concentration causing half-maximal stimulation; IC₅₀, concentration causing half-maximal inhibition; k_{+1} , association rate constant; $k_{−1}$, dissociation rate constant; PAGE, polyacrylamide gel electrophoresis; p-gp, p-glycoprotein; SDS, sodium dodecyl sulfate.

tion with cytotoxic drugs (Ferry et al., 1992). Moreover, it would enable a more straightforward analysis of the effects of single mutations on drug-p-gp interactions than photolabeling.

Here we report the synthesis and characterization of a novel photoreactive DHP, BZDC-DHP, that photoincorporates into p-gp. It inhibits drug transport at lower concentrations than azidopine. The tritiated derivative can be also used to reversibly label a chemosensitizer binding domain on p-gp in multidrug-resistant cells with low nanomolar K_d . This site is distinct from the vinblastine receptor domain. Our structure-function relationship of several DHPs suggests that, unlike for the DHP binding domain of L-type Ca^{2+} channels (Glossmann & Striessnig, 1990), the DHP moiety does not determine site selectivity on p-gp.

MATERIALS AND METHODS

Materials. Protein A-Sepharose, bovine serum albumin, and protease inhibitors were from Sigma Chemical Co. (Deisenhofen, Germany). Unlabeled Ca^{2+} antagonists were kindly provided by Dr. Traut (Knoll AG, Ludwigshafen, Germany) and Sandoz AG (Basel, Switzerland).

Synthesis of (\pm)-BZDC-DHP and ($-$)-[^3H]BZDC-DHP. Unlabeled and tritiated (≈ 50 Ci/mmol) *N*-hydroxysuccinimidyl-BZDC were prepared as described previously (Olszewski et al., 1995; Mourey et al., 1993). To synthesize unlabeled (\pm)-BZDC-DHP, *N*-hydroxysuccinimidyl-BZDC was coupled to the free amino group of the racemic DHP precursor previously used to synthesize azidopine (Striessnig et al., 1986). All reactions were performed under yellow light. The free base of the DHP amino precursor was prepared by adding 0.1 mL of 10 N NaOH to 3 μmol of precursor followed by extraction into 3 \times 0.1 mL of ethyl acetate. A 5 mg (1.4 μmol) amount of *N*-hydroxysuccinimidyl-BZDC dissolved in 50 μL of dimethylformamide was added to the extract, and the mixture was incubated for 60 min on ice. The extraction mixture was then separated on a Silica Gel 60 thin-layer plate (20 \times 20 cm) developed with diethyl ether/ethyl acetate (70/30). This allowed the efficient separation of the amino precursor ($R_f < 0.05$, $n = 5$) and uncoupled *N*-hydroxysuccinimidyl-BZDC ($R_f > 0.7$, $n = 4$) from the reaction product, (\pm)-BZDC-DHP ($R_f = 0.26 \pm 0.03$, $n = 4$). (\pm)-BZDC-DHP was eluted into 0.5 mL of ethanol and stored in the dark at -25°C . To synthesize ($-$)-[^3H]BZDC-DHP, 0.5 mCi of *N*-hydroxysuccinimidyl-[^3H]BZDC was added to 3 μmol of the ($-$)-enantiomer of the DHP precursor extracted into ethyl acetate as above. After incubation and separation the radioactive peaks were detected using a Berthold TLC analyzer. The product peak contained more than 95% of the total radioactivity on the thin-layer plate. After elution into ethanol more than 50% ($n = 3$) of the total radioactivity employed was recovered as ($-$)-[^3H]BZDC-DHP.

Membrane Preparation and Reversible Binding Assay. The T-lymphoblastoid cell line CCRF-CEM was obtained from American Type Culture Collection. Multidrug-resistant subline CCRF-ADR5000 or CCRF-VCR1000 cells and the nonresistant cells (CCRF-CEM) were cultured as described (Borchers et al., 1995). Cell membrane fragments were prepared as reported elsewhere (Borchers et al., 1995), resuspended in 10 mM Tris-HCl, pH 7.4, 50% (v/v) glycerol, 10 mM NaCl, 1.5 mM MgCl_2 at a final protein concentration of 3–10 mg/mL and stored in small aliquots at -85°C until use. For binding and photolabeling experiments membranes

were diluted (usually 10–20-fold) into assay buffer (50 mM Tris-HCl, pH 7.4, at 37°C , 0.1 mM phenylmethylsulfonyl fluoride) and subjected to a freeze-thaw cycle (quick freeze in liquid nitrogen followed by thawing at room temperature). This facilitates equilibration of assay buffer into the vesicles thus excluding drug accumulation phenomena due to differences, e.g., in pH. ATP was excluded from the buffer to prevent active drug transport by p-gp. To measure saturable binding ($-$)-[^3H]BZDC-DHP was incubated for 60 min (25°C or on ice) with membrane protein in assay buffer (0.5 mL final volume). Nonspecific binding was determined in the presence of 1 μM (\pm)-BZDC-DHP or 1 μM cyclosporin A. Bound ligand was determined by rapid dilution of the incubation mixture with 4 mL of filtration buffer [10% (w/v) polyethylene glycol 6000, 10 mM Tris-HCl, pH 7.4, 10 mM MgCl_2] followed by rapid filtration over GF/C Whatman glass fiber filters. Filters were washed three times with filtration buffer, and bound radioactivity was determined by liquid scintillation counting.

Membrane protein concentrations were determined according to Lowry et al. (1951) using bovine serum albumin as a standard.

[^3H]Vinblastine binding was carried out according to Ferry et al. (1992) employing K_d concentrations of radioligand (40 nM).

Photoaffinity Labeling. For photoaffinity labeling of p-gp with ($-$)-[^3H]BZDC-DHP or [^3H]azidopine, membranes were incubated with the respective ligand for 60 min at 25°C . Ligand and protein concentrations are given in the figure legends. Samples were chilled on melting ice, and 50 μL aliquots were removed to determine reversible binding. The samples were then transferred to plastic petridishes and irradiated with ultraviolet light. The photolysis conditions were optimized for the two photoligands (not shown) and were as follows: [^3H]azidopine-labeled membranes were irradiated for 20 min with a Camag (Berlin, Germany) 366 nm ultraviolet lamp (10 cm distance). ($-$)-[^3H]BZDC-DHP-labeled membranes were irradiated for 2 h with a Philips TL30 black light lamp (5 cm distance). After photolysis, aliquots of the irradiation mixtures were denatured in electrophoresis sample buffer containing 10 mM dithiothreitol or 2% (v/v) β -mercaptoethanol and separated by SDS-PAGE (8% polyacrylamide). Radioactive bands were visualized by fluorography or after gel slicing as described previously (Moebius et al., 1993; Borchers et al., 1995).

Immunological Techniques. Polyclonal sequence-directed antibodies anti-p-gp₃₈₉ and anti-p-gp₉₀₉ were raised in rabbits against synthetic peptides corresponding to amino acids 389–406 and 909–926, respectively. For immunoprecipitation, photolabeled CCRF-ADR5000 membranes (0.2–0.3 mg of protein/mL) in binding buffer were solubilized by addition of SDS to a final concentration of 2% (w/v). The sample was incubated for 30 min at 25°C and then boiled for 3 min. The mixture was diluted 10-fold with RIA buffer [50 mM Tris-HCl, pH 7.4, 0.15 M NaCl, 0.5 mg of bovine serum albumin/mL, 1% (v/v) Triton X100]. After 30 min of incubation on ice, insoluble material was removed by centrifugation (12 500g, 10 min). Solubilized protein was incubated overnight at 4°C with Protein A-bound antibodies. The Protein A-Sepharose was washed four times with 1.5 mL of ice-cold RIA buffer. Bound radioactivity was determined by liquid-scintillation counting of the washed Sepharose pellet.

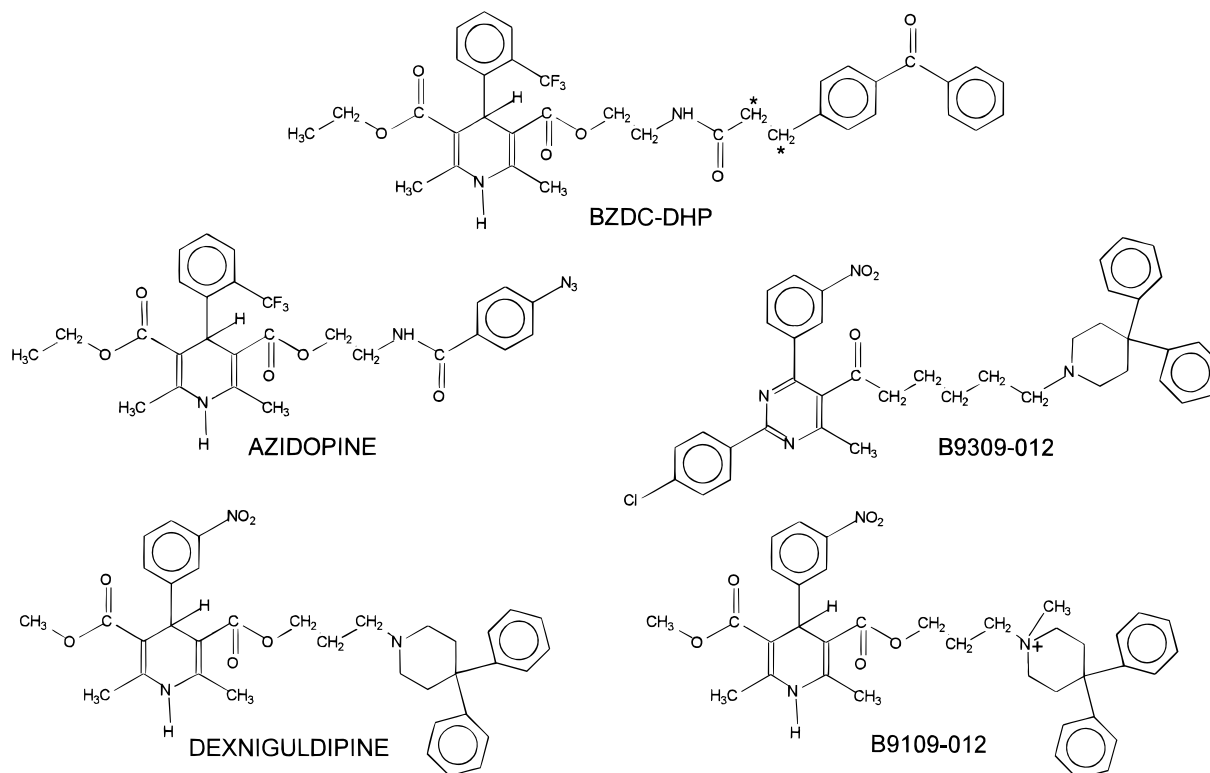


FIGURE 1: Chemical structures of azidopine-related chemosensitizers BZDC-DHP, azidopine, dexniguldipine, quaternary dexniguldipine (B9109-012), and B9309-012. The positions of the tritium labels on BZDC-DHP are indicated by asterisks.

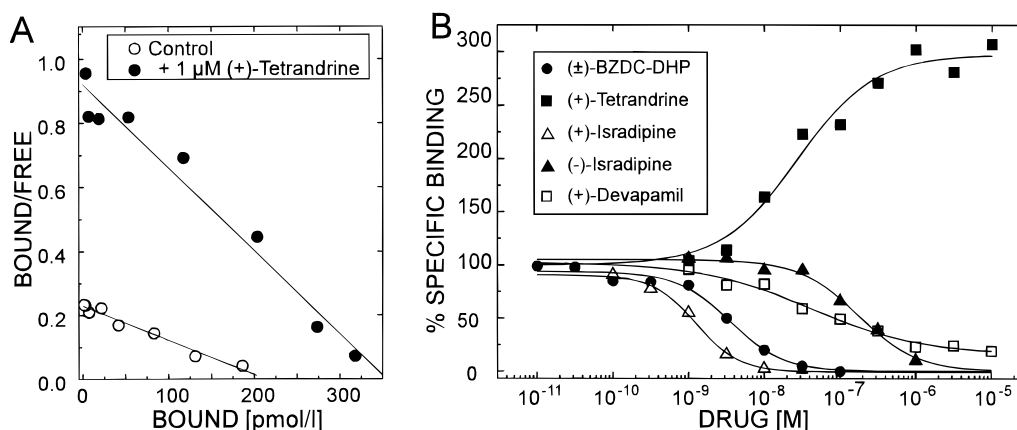


FIGURE 2: High-affinity interaction of (–)-[3 H]BZDC-DHP with skeletal muscle L-type Ca^{2+} channels. (A) Saturation analysis: Increasing concentrations of (–)-[3 H]BZDC-DHP were incubated with 0.048 mg of skeletal muscle microsomes/mL (60 min, 37 °C) in the absence and presence of 1 μ M (+)-tetrandrine. Nonspecific binding [in the presence of 1 μ M (±)-isradipine] was subtracted from total binding to yield specific binding. A Scatchard transformation of the binding data is shown. The following binding parameters were determined by linear regression analysis: control, $K_D = 0.94$ nM, $B_{\text{max}} = 214$ pmol/L (3.7 pmol/mg of protein); with 1 μ M (+)-tetrandrine: $K_D = 0.38$ nM, $B_{\text{max}} = 354$ pmol/L (6.1 pmol/mg of protein). (B) Binding modulation by unlabeled Ca^{2+} antagonists: 0.8 nM (–)-[3 H]BZDC-DHP was incubated with 0.017 mg of skeletal muscle microsomes/mL in the absence (control) or presence of increasing concentrations of unlabeled drugs. Specific binding in the presence of drug is expressed as percent of control (0.7 pmol/mg of protein). The following binding parameters were obtained by nonlinear curve-fitting (given as IC_{50} , slope factor, % maximal inhibition): (±)BZDC-DHP, 3.3 nM, 1.18, 100%; (+)-isradipine, 1.1 nM, 1.23, 100%; (–)-isradipine, 178 nM, 1.16, 100%; (+)-devapamil, 43 nM, 0.62, 84%. (+)-Tetrandrine was stimulatory: $\text{EC}_{50} = 24$ nM, slope = 0.80, maximal stimulation to 298% of control binding. The following K_i values were calculated for competitive inhibitors according to Linden (1982): (±)-BZDC-DHP, 1.9 nM; (+)-isradipine, 0.7 nM; (–)-isradipine, 97 nM.

Immunoblot analysis was carried out as described previously (Moebius et al., 1994).

Rhodamine 123 Accumulation Assay. Inhibition of rhodamine 123 accumulation by chemosensitizers was determined at pH 7.3 as described previously in CCRF-VCR1000 cells (Borchers et al., 1995; Boer et al., 1994).

Data Analysis. Binding inhibition (or stimulation) curves were fitted to the general dose-response equation (DeLean et al., 1978) to determine IC_{50} (or EC_{50}) values and slope factors. Association kinetics were fitted to the differential form of the second-order rate equation using nonlinear least

square fitting to determine k_{+1} and k_{-1} . Data are given as mean \pm SE for the indicated number of experiments.

RESULTS

Development of BZDC-DHP as a Photoreactive Probe. To develop a sensitive assay for the reversible labeling of a chemosensitizer interaction site on the p-gp we synthesized the tritiated Ca^{2+} antagonist (–)-[3 H]BZDC-DHP as a novel probe. Its chemical structure is depicted in Figure 1. It is structurally closely related to azidopine, a chemosensitizer

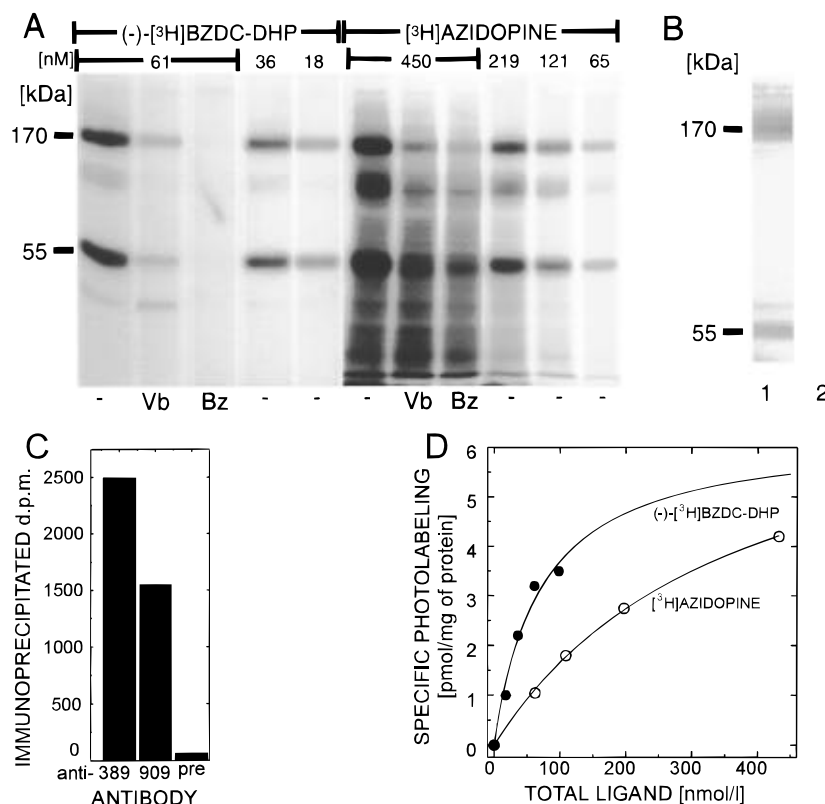


FIGURE 3: Photolabeling of p-gp with (–)-[³H]BZDC–DHP and [³H]azidopine. (A) Fluorography: 0.25 mg of CCRF-ADR5000 membrane protein/mL was incubated in the dark with the indicated concentrations of (–)-[³H]BZDC–DHP or [³H]azidopine in the absence or presence of 5 μM vinblastine (Vb) or 10 μM (±)-BZDC–DHP (Bz). Reversible (–)-[³H]BZDC–DHP binding (given in legend to panel D) was determined in 0.05 mL aliquots (duplicate determinations) by rapid filtration (see Materials and Methods). Aliquots (0.05 mL) of all samples were then transferred to 96-well microtiter plates and irradiated with ultraviolet light on ice as described in Materials and Methods. Aliquots (40 μL, 0.010 mg of protein) were denatured in SDS–PAGE sample buffer and separated on 8% polyacrylamide gels together with prestained marker proteins. Incorporated radioactivity was either visualized by fluorography of the dried gel or by quantification of the incorporated radioactivity in 1 mm slices of a gel run in parallel with the same samples (see panel D). The migration of p-gp (170 kDa) and a labeled proteolytic fragment (55 kDa) are indicated. (B) Immunoblot: CCRF-ADR5000 membranes (~0.01 mg/lane) were separated as in A and electroblotted to a PVDF-membrane. Immunostaining was carried out with affinity-purified anti-p-gp₉₀₉. Staining was completely prevented after preincubation of the antibody with 1 μM antigenic synthetic peptide (lane 2). (C) Immunoprecipitation: CCRF-ADR5000 membranes were photolabeled as described in A. Aliquots (50 μL, 4500 dpm photolabeled p-gp) were solubilized in SDS, diluted in RIA buffer, and immunoprecipitated (50 μL serum) with anti-p-gp₃₈₉ (anti-389), anti-p-gp₉₀₉ (anti-909), or preimmune serum (pre) as described in Materials and Methods. (D) Quantitative analysis of a photolabeling experiment conducted as shown in panel A. Incorporated ligand was determined in 1 mm gel slices. Nonspecific labeling [in the presence of 10 μM (±)-BZDC–DHP] was subtracted from total labeling to yield specific labeling. Specific labeling (in pmol/mg of protein) is plotted against total ligand concentration. Reversible (–)-[³H]BZDC–DHP binding before photolysis was as follows: 18 nM ligand, 21 pmol/mg; 36 nM ligand, 30 pmol/mg; 61 nM ligand, 54 pmol/mg; 96 nM ligand, 54 pmol/mg. From these values we calculated a photolabeling efficiency [(dpm photolabeling/dpm reversibly bound) × 100] of 12%–18%.

and potent L-type Ca²⁺ channel blocker. From the known structure-activity relationships, we predicted that replacement of azidopine's photoreactive phenyl azide substituent in position C3 by a benzophenone moiety should increase its affinity for the p-gp without major changes in Ca²⁺ channel affinity. Figure 2 shows that this is indeed the case. (–)-[³H]BZDC–DHP reversibly binds to Ca²⁺ channels in skeletal muscle microsomes with subnanomolar *K_d* (0.5–0.9 nM, *n* = 2) and a *B_{max}* of 3.0–3.7 pmol/mg of protein (*n* = 2). Binding was modulated by other chemical classes of Ca²⁺ antagonists with pharmacological profiles indistinguishable from [³H]azidopine [cf. data in Figure 2B with data for [³H]azidopine in (Striessnig et al., 1986)]. As expected for Ca²⁺ channel labeling, (+)-tetrandrine (Glossmann & Striessnig, 1990) was a positive allosteric modulator, increasing equilibrium (–)-[³H]BZDC–DHP binding in a concentration-dependent manner (Figure 2A,B). (–)-[³H]BZDC–DHP specifically photolabeled (not shown) the purified channel's α1 subunit with labeling yields (16% ± 5%, *n* = 3,) similar to those reported for [³H]-azidopine (Striessnig et al., 1986). Due to the well-established advantages of the photoreactive benzophenone moiety

(BZDC–DHP) over phenyl azides (like azidopine) (Olszewski et al., 1995), (–)-[³H]BZDC–DHP represents a DHP photoaffinity probe for L-type Ca²⁺ channels that is superior to [³H]azidopine.

(–)-[³H]BZDC–DHP Photolabels p-gp. The higher activity of (–)-[³H]BZDC–DHP for the proposed DHP binding domain on p-gp was evident from photoaffinity labeling experiments using the multidrug-resistant human lymphoblastoid cell line CCRF-ADR5000. This cell line expresses high densities of wild type p-gp (glycine in position 185; V. Gekeler, personal communication). Increasing concentrations of (–)-[³H]BZDC–DHP (18–61 nM) and [³H]azidopine (65–450 nM) were incubated for 60 min with 0.25 mg of membrane protein/mL. The incubation was carried out in the absence of ATP to preclude p-gp-mediated drug accumulation into inside-out vesicles. The incubation mixtures were then photolyzed, and the labeled membranes were separated by SDS–PAGE. The majority of saturable (–)-[³H]BZDC–DHP (and [³H]azidopine) photolabeling occurred into polypeptides with apparent molecular masses of 170, 95, and 55 kDa (Figure 3A). Photolabeling was completely protected by 10 μM unlabeled ligand and partially

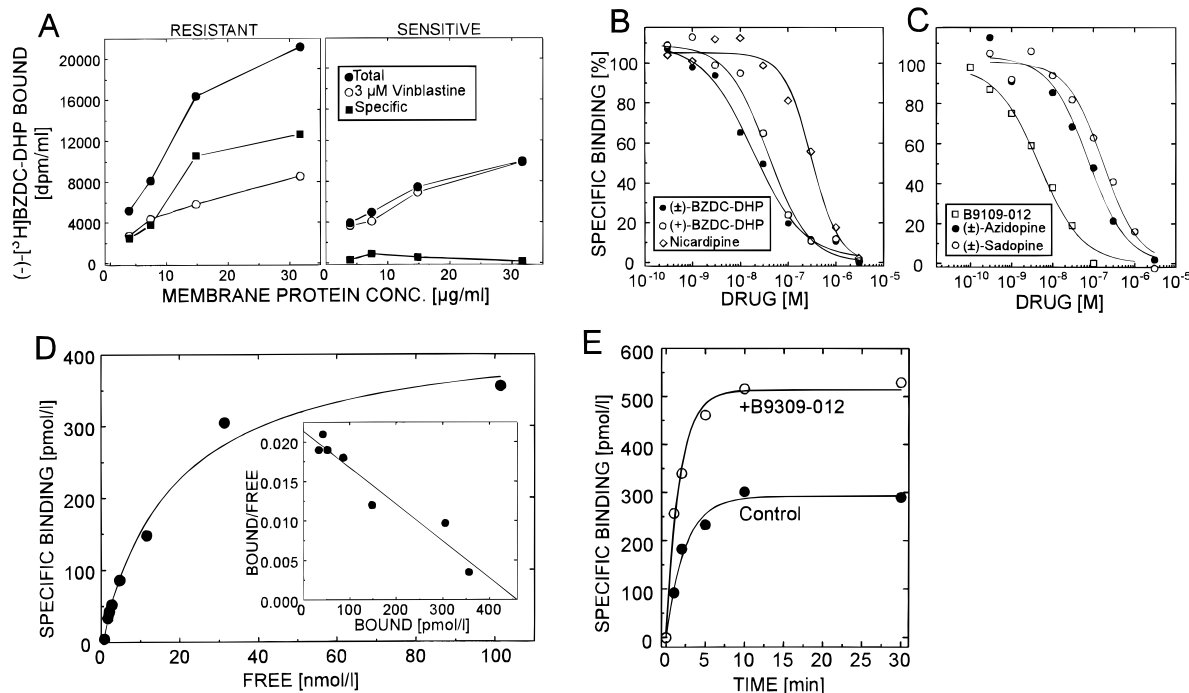


FIGURE 4: Reversible binding properties of (-)-[³H]BZDC-DHP to p-gp. (A) Protein concentration dependent binding: 0.9 nM (-)-[³H]BZDC-DHP was incubated (60 min, 25 °C) with increasing concentrations of microsomal membranes prepared from resistant (ADR5000) or sensitive (CCRF-CEM) cells. Incubations were carried out in the absence or presence of 3 μM vinblastine or 3 μM (±)-BZDC-DHP. Bound ligand was measured by rapid filtration of the samples through GF/C glass fiber filters (see Materials and Methods). One of three experiments yielding similar results is shown. (B, C) Inhibition by DHPs: 0.4–1.7 nM (-)-[³H]BZDC-DHP was incubated with CCRF-ADR5000 membrane protein (0.06–0.012 mg/mL) in the absence (control binding) or presence of increasing concentrations of the indicated drugs. Nonspecific binding [in the presence of 3 μM (±)-BZDC-DHP] was subtracted from total binding to yield specific binding. Specific binding in the presence of drugs is expressed as percent of control (1.9–14 pmol/mg of protein). The following binding parameters (given as IC₅₀, slope factor) were obtained by nonlinear curve fitting for the experiments shown (for statistics see text and Table 1): (±)-BZDC-DHP, 18.8 nM, 0.82; (+)-BZDC-DHP, 38 nM, 1.02; nicardipine, 306 nM, 1.490; B9109-012, 4.8 nM, 0.82; (±)-azidopine, 75 nM, 0.91; (±)-sadopine, 172 nM, 0.99. (D) Saturation analysis: 1.2 nM of (-)-[³H]BZDC-DHP was incubated with CCRF-ADR5000 membrane protein (0.006 mg/mL) in the absence and presence of increasing concentrations of unlabeled (±)-BZDC-DHP. From the inhibition curve a binding isotherm was calculated taking into account the isotopic dilution of the radioligand. Specific binding was 3726 dpm in the absence and 650 dpm in the presence of 100 nM unlabeled drug. The following binding parameters were calculated from a Scatchard transformation of the saturation binding data (inset): K_D = 21 nM, B_{max} = 458 pM (74 pmol/mg of protein). (E) Association kinetics: 3.4 nM (-)-[³H]BZDC-DHP was incubated with CCRF-ADR5000 membrane protein (0.016 mg/mL, receptor concentration = 0.85 nM) at 2 °C with and without (control) 500 nM B9309-012. After the indicated incubation periods the specific binding was determined by rapid filtration. The observed association rates (*k*_{obs}) were 0.41 min⁻¹ (control) and 0.59 min⁻¹ (B9309-012 present). From the association time course of the control experiment, the following kinetic constants were calculated by nonlinear curve fitting the data to the second-order rate equation: *k*₊₁ = 0.045 nM⁻¹ min⁻¹; *k*₋₁ = 0.241 min⁻¹; K_D = 5.4 nM.

protected by 5 μM vinblastine. The three polypeptides represent p-gp (170 kDa) as well as two of its previously described (Borchers et al., 1995; Yoshimura et al., 1989) proteolytic fragments (95 and 55 kDa). For the two major labeled bands (p-gp and the 55 kDa fragment) this was confirmed by immunoblot analysis (Figure 3B) with sequence-directed antibodies. Antibody anti-p-gp₉₀₉, directed against a cytoplasmic loop close to the C-terminal end of p-gp, selectively recognized the 170 and 55 kDa peptides. Moreover, this antibody, as well as anti-p-gp₃₈₉, specifically immunoprecipitated (-)-[³H]BZDC-DHP-labeled p-gp (Figure 3C). Minor labeling of a 35–38 kDa fragment, observed at the highest (-)-[³H]BZDC-DHP concentrations (Figure 3A), was not sensitive to vinblastine and may therefore represent a polypeptide unrelated to p-gp (see also Borchers et al., 1995).

Fluorography (Figure 3A) as well as quantitative analysis of p-gp photolabeling (Figure 3D) revealed that about 5 times lower concentrations of (-)-[³H]BZDC-DHP were required to obtain similar photoincorporation as compared to [³H]-azidopine. This also explains the lower background labeling observed for (-)-[³H]BZDC-DHP (Figure 3A) and suggests that (-)-[³H]BZDC-DHP displays significantly higher affinity for p-gp than [³H]azidopine.

(-)-[³H]BZDC-DHP Is a Reversible Label for p-gp. Its higher affinity and low background prompted us to investigate whether (-)-[³H]BZDC-DHP could be used to reversibly label its binding domain on p-gp in a specific manner. (-)-[³H]BZDC-DHP was incubated for 60 min with increasing concentrations of membrane protein prepared from resistant and sensitive cells under conditions preventing drug accumulation into inside-out vesicles (i.e., in the absence of ATP). Figure 4 shows that total (-)-[³H]BZDC-DHP binding was about 2 times higher in resistant cells. Inclusion of 3 μM vinblastine in the incubation mixture reduced binding to the level observed in sensitive cells at all protein concentrations examined. Saturable binding was not dependent on temperature as similar results were obtained after incubation at 2 or 25 °C, respectively (not shown). Therefore a vinblastine-sensitive (-)-[³H]BZDC-DHP binding component exists in resistant cells but not in sensitive cells. As (-)-[³H]BZDC-DHP specifically photolabels only p-gp and fragments thereof in a vinblastine-sensitive manner in CCRF-ADR5000 membranes, the reversibly labeled site must also be located on p-gp.

To further confirm this assumption we analyzed the potency of various DHPs, structurally unrelated chemosensitizers, and cytotoxic drugs for their ability to compete with

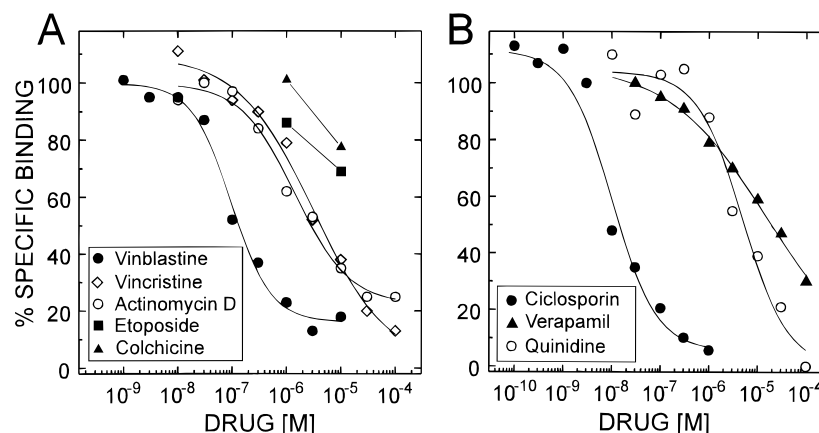


FIGURE 5: Inhibition of reversible $(-)-[^3\text{H}]\text{BZDC-DHP}$ binding by p-gp active drugs. Experimental conditions were as in Figure 4B,C. The following binding parameters (given as IC_{50} , slope factor, % maximal inhibition) were calculated by nonlinear curve fitting of the data. (A) Cytotoxic drugs: vinblastine, 96 nM, 1.18, 84%; vincristine, 3.14 μM , 0.63, 100%; actinomycin D, 1.4 μM , 0.87, 78%. (B) Cyclosporin A, 10.2 nM, 0.96, 100%, (\pm)-verapamil, 14.6 μM , 0.43 (assuming complete inhibition); quinidine, 4.9 μM , 0.93, 100%.

Table 1: Inhibition of $(-)-[^3\text{H}]\text{BZDC-DHP}$ Binding to ADR5000 Membranes^a

drug	IC_{50} (nM)	slope factor	maximal inhibition (%)
(\pm)-BZDC-DHP	12.6 \pm 1.9	0.96 \pm 0.09	100
(+)-BZDC-DHP	38–49	0.98–1.02	100
(\pm)-azidopine	105 \pm 23	0.98 \pm 0.08	100
(\pm)-sadopine	172–226	0.99–1.00	100
nicardipine	213 \pm 50	1.02 \pm 0.25	100
B9109-012	7.2 \pm 2.2	0.92 \pm 0.05	100
vinblastine	54 \pm 13	0.90 \pm 0.10	93 \pm 2.6
vincristine	4100 \pm 1200	0.77–0.09	100
actinomycin D	1400–4200	0.68–0.87	19–22
colchicine	>10000	nd ^b	nd
etoposide	>10000	nd	nd
cyclosporin A	3.7 \pm 1.8	1.19 \pm 0.12	97.5 \pm 2.1
quinidine	2800 \pm 960	0.66 \pm 0.13	100
verapamil	14600 \pm 2100	0.53 \pm 0.10	100 ^c
dexniguldipine	10.5 \pm 3.6		100
	(48% \pm 7% of sites)		
	1900 \pm 540		
	(52% of sites)		
niguldipine	stimulation	nd	
B9309-012	stimulation	nd	
prenylamine	stimulation	nd	

^a Binding experiments were performed and analyzed as described in Methods and legends to Figures 4, 5, and 7. Data are given as means \pm SE from at least three experiments or as a range from two experiments. Percent inhibition is defined as 100 – (% of control binding in the presence of drug). ^b nd, not determined. ^c Data were calculated assuming maximal inhibition to 100%.

$(-)-[^3\text{H}]\text{BZDC-DHP}$ binding. As shown in Figure 4B,C and Table 1, (\pm)-BZDC-DHP was among the most potent inhibitors (IC_{50} = 12.6 \pm 1.9 nM, n = 9). The (+)-enantiomer was slightly less active (IC_{50} = 38–49 nM, n = 2). In accordance with the photolabeling experiments, (\pm)-azidopine was about 5 times less potent (IC_{50} = 105 \pm 23 nM, n = 3) as was the azidopine-related DHP (\pm)-sadopine (Knaus et al., 1992) (IC_{50} = 172–226 nM, n = 2). Nicardipine (IC_{50} = 213 \pm 50 nM, n = 3) and the quaternary dexniguldipine derivative B9109-012 (IC_{50} = 7.2 \pm 2.2 nM, n = 3; for chemical structure see Figure 1) also displayed IC_{50} values in the nanomolar range (Table 1).

Estimates for the $(-)-[^3\text{H}]\text{BZDC-DHP}$ equilibrium binding parameters were obtained from experiments in which the specific radioactivity of the ligand was decreased with increasing concentrations of unlabeled (\pm)-BZDC-DHP. Assuming equal affinity for both BZDC-DHP enantiomers a K_d value of 16.3 \pm 4.6 nM and a B_{max} of 56 \pm 12 pmol/

mg of protein (n = 4) was calculated (Figure 4D). These B_{max} estimates are in accordance to the density of p-gp reported in multidrug-resistant cells (31–140 pmol/mg of protein) (Ferry et al., 1992; Cornwell et al., 1986, 1987; Jaffrezou et al., 1991).

The high binding affinity for the $(-)-[^3\text{H}]\text{BZDC-DHP}$ –p-gp interaction was confirmed by measuring the association time course (Figure 4E). At ligand concentrations $\ll K_d$, binding equilibrium was reached within 10 min at 22 °C. Using the differential form of the second-order rate equation, association and dissociation rate constants of k_{+1} = 0.031 nM⁻¹ min⁻¹ (0.018–0.045, n = 2) and k_{-1} = 0.172 min⁻¹ (0.167–0.177, n = 2) were calculated, respectively. This yields a kinetically derived K_d ($= k_{-1}/k_{+1}$) of 7.6 (5.4–9.7, n = 2) nM, in close agreement with the K_D from our equilibrium studies.

$(-)-[^3\text{H}]\text{BZDC-DHP}$ binding was also inhibited by DHP unrelated compounds. From the cytotoxic drugs (Figure 5A) investigated, vinblastine was the most potent blocker (IC_{50} = 54 \pm 13 nM, n = 6) causing incomplete inhibition to 7% \pm 2.6% (n = 6) of control binding. In accordance with its lower affinity for the [^3H]vinblastine binding domain (Ferry et al., 1992) vincristine was >50 times less potent (IC_{50} = 4.1 \pm 1.2 μM , n = 4), as was actinomycin D (Figure 5A, Table 1). Colchicin and etoposide were weak inhibitors (IC_{50} > 10 μM). Cyclosporin A, known as a highly potent chemosensitizer (Foxwell et al., 1989), caused complete inhibition with an IC_{50} of 3.7 \pm 1.8 nM (n = 5) (Figure 5B). Drugs reported to represent weaker transport inhibitors, like verapamil and quinidine, displayed >100 times lower affinity for $(-)-[^3\text{H}]\text{BZDC-DHP}$ -labeled p-gp (Figure 5B, Table 1).

This reversible labeling profile was in agreement with the modulation of p-gp photolabeling by $(-)-[^3\text{H}]\text{BZDC-DHP}$: 3 μM vinblastine partially protected reversible binding and photolabeling (cf., Figures 3A and 5A), whereas 200 nM cyclosporin A caused almost complete protection of both (not shown). Moreover, reversible $(-)-[^3\text{H}]\text{BZDC-DHP}$ binding before ultraviolet irradiation correlated with the amount of specific photolabeling recovered in the p-gp-associated peptides after SDS–PAGE (see legend to Figure 3D). Taken together these results unequivocally demonstrate that $(-)-[^3\text{H}]\text{BZDC-DHP}$ reversibly binds to a chemosensitizer binding domain on p-gp with high affinity.

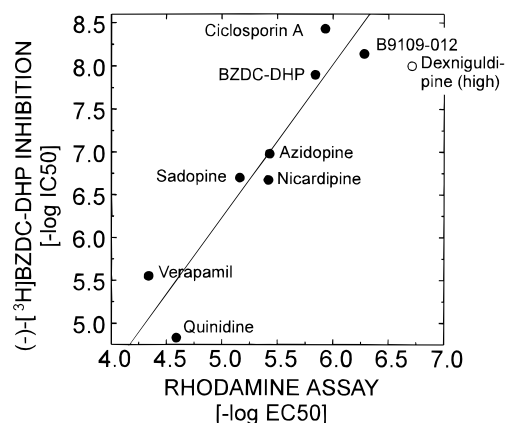


FIGURE 6: Correlation of $(-)-[^3\text{H}]\text{BZDC-DHP}$ binding inhibition potency with energy-dependent drug transport inhibition. The effect of the chemosensitizers tested in the binding assays on rhodamine 123 accumulation was measured in the multidrug-resistant CCRF-CEM subline VCR1000 as described in Materials and Methods. All drugs dose dependently reversed the decreased rhodamine 123 accumulation (15%–25% of the accumulation level of sensitive cells) in multidrug-resistant VCR1000 cells to the values observed in the sensitive cells. EC_{50} values for reversal were calculated as the mean from three independent experiments. The negative log of the EC_{50} (varying less than 10%) is plotted against the negative log of the mean IC_{50} values (for statistics see text) for $(-)-[^3\text{H}]\text{BZDC-DHP}$ binding inhibition. The linear regression line is defined as $y = -2.684 + 1.784x$, $r = 0.94$, $n = 8$. Data from B9309-012, niguldipine (binding stimulators), and dexniguldipine (biphasic inhibitor) were not included in the regression analysis. Open circle: high-affinity binding component of dexniguldipine.

To determine whether the drug potencies for $(-)-[^3\text{H}]\text{BZDC-DHP}$ binding inhibition correlate with the potency for the inhibition of energy-dependent drug transport by p-gp, we measured transport inhibition using rhodamine 123 accumulation. The resulting EC_{50} values for reversal of decreased rhodamine 123 accumulation were then plotted against the IC_{50} values for drug binding inhibition (Figure 6). Concentrations for inhibition of drug transport were higher than for binding inhibition. Nevertheless, the high correlation ($r = 0.94$, $n = 8$) demonstrates that reversible $(-)-[^3\text{H}]\text{BZDC-DHP}$ binding can identify potent blockers of p-gp-mediated drug transport.

BZDC-DHP almost completely reverted resistance of ADR5000 cells to vincristine, with a half-maximal effect occurring at $5 \mu\text{M}$ (data not shown).

$(-)-[^3\text{H}]\text{BZDC-DHP}$ Binding Is Stimulated by Certain DHP Derivatives. Dexniguldipine (the minus enantiomer

of the potent Ca^{2+} channel blocker niguldipine) represents an azidopine-related DHP with potent chemosensitizing properties (Hofmann et al., 1992; Reymann et al., 1993; Boer et al., 1994). In contrast to azidopine and BZDC-DHP, dexniguldipine carries a 4,4-diphenylpiperidinyl moiety on the C3 substituent. Figure 7A illustrates the effects of dexniguldipine and its (+)-enantiomer (niguldipine) on $(-)-[^3\text{H}]\text{BZDC-DHP}$ binding to p-gp. Unexpectedly, both enantiomers displayed a complex interaction with the $(-)-[^3\text{H}]\text{BZDC-DHP}$ -labeled site. Dexniguldipine inhibited in a biphasic manner with apparent IC_{50} values of $10.5 \pm 3.6 \text{ nM}$ ($48\% \pm 7\%$ of sites) and $1.9 \pm 0.54 \mu\text{M}$ (52% of sites) ($n = 4$). In contrast, low nanomolar concentrations of the (+)-enantiomer (niguldipine) stimulated $(-)-[^3\text{H}]\text{BZDC-DHP}$ binding to $170\% \pm 2\%$ ($n = 4$) of control binding, whereas concentrations above $1 \mu\text{M}$ were inhibitory. High-affinity inhibition by dexniguldipine and stimulation by niguldipine occurred within a similar concentration range. As evident from Figure 6 the high-affinity component of dexniguldipine agreed well with its potency for rhodamine 123 transport inhibition (open circle in Figure 6). Quaternarization of dexniguldipine's basic nitrogen completely eliminated the low-affinity component (Figure 4) and yielded B9109-012, a potent and complete blocker of $(-)-[^3\text{H}]\text{BZDC-DHP}$ binding. Quaternarization only slightly decreased the potency (2.7-fold) for the inhibition of drug transport (Figure 6). This indicates that the permanently charged B9109-012 binds to an extracellular site on p-gp or has access to an intracellular site in our resistant cells (e.g., through active transport) despite its permanent charge.

Stimulation of $(-)-[^3\text{H}]\text{BZDC-DHP}$ binding was even more pronounced by another dexniguldipine-related compound, B9309-012. In B9309-012 (Figure 1) the substituted DHP ring is eliminated by ring introduction of a nitrogen atom and addition of a bulky chlorophenyl ring. Submicromolar concentrations of B9309-012 stimulated $(-)-[^3\text{H}]\text{BZDC-DHP}$ equilibrium binding up to 400% (Figure 7B) in a dose-dependent manner. Because concentrations above $1 \mu\text{M}$ also increased nonspecific DHP binding (not shown), we did not perform a complete analysis of its dose-response curve. 500 nM B9309-012 was without major effect on the association time course of $(-)-[^3\text{H}]\text{BZDC-DHP}$ (Figure 4E). Stimulation by niguldipine and B9309-012 was not additive because the stimulatory but not the inhibitory component of niguldipine (Figure 7A) was eliminated in the presence of

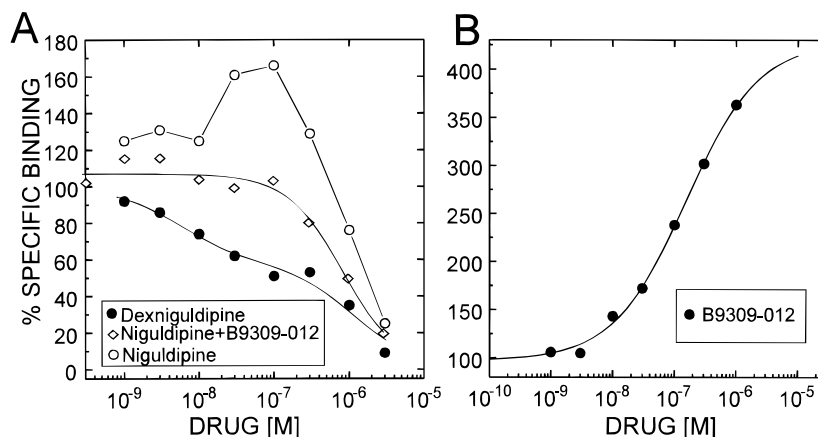


FIGURE 7: Modulation of $(-)-[^3\text{H}]\text{BZDC-DHP}$ binding to p-gp by the niguldipine enantiomers. Experimental conditions were as in Figure 4B,C. Niguldipine modulation was also measured for $(-)-[^3\text{H}]\text{BZDC-DHP}$ binding stimulated by 500 nM B9309-012 (diamonds). The following binding parameters were calculated for dexniguldipine (panel A, assuming 100% inhibition): single-site fit, $\text{IC}_{50} = 140 \text{ nM}$, slope factor = 0.44; two-site fit, site 1, $\text{IC}_{50} = 5.7 \text{ nM}$ (58% of sites), and site 2, $\text{IC}_{50} = 1.1 \mu\text{M}$ (42% of sites).

500 nM B9309-012. The high-affinity component of dextran-goldipine inhibition remained almost unchanged ($IC_{50} = 11\text{--}12$ nM, 35%–40% of sites) in the presence of B9309-012.

To test whether stimulation of $(-)-[^3H]BZDC\text{--}DHP$ binding is due to an increase in binding affinity or an increase in the apparent B_{max} , we measured the effect of 500 nM B9309-012 on the IC_{50} of $(\pm)\text{--}BZDC\text{--}DHP$. Although this concentration of B9309-012 caused a 2–3-fold stimulation of specific binding, only a small, not statistically significant decrease in the IC_{50} of $(\pm)\text{--}BZDC\text{--}DHP$ (8.3 ± 1.5 nM, $n = 3$) was found. This implies that the stimulatory effect is mainly caused by an increase in the apparent number of binding sites for the radioligand. In contrast, 500 nM B9309-012 significantly ($p < 0.05$) decreased the apparent potency of vinblastine for $(-)-[^3H]BZDC\text{--}DHP$ inhibition by about 10-fold ($IC_{50} = 403 \pm 155$ nM, $n = 3$). The differential effect of B9309-012 on the apparent affinity of BZDC–DHP and vinblastine demonstrates that separate sites are labeled by BZDC–DHP and vinblastine.

We also tested the effect of the phenylalkylamine prenylamine, which has been reported to stimulate $[^3H]$ azidopine photolabeling (Fleming et al., 1992). Prenylamine also stimulated $(-)-[^3H]BZDC\text{--}DHP$ binding in a stereoselective manner. The $(+)$ -enantiomer was a more potent stimulator ($1\text{ }\mu\text{M}$, to $407\% \pm 40\%$; $10\text{ }\mu\text{M}$, to $502\% \pm 69\%$ of control binding; $n = 3$) than the respective $(-)$ -enantiomer ($1\text{ }\mu\text{M}$, to $212\% \pm 18\%$; $10\text{ }\mu\text{M}$, to $276\% \pm 2\%$ of control binding; $n = 3$).

In contrast to $(-)-[^3H]BZDC\text{--}DHP$, B9309-012 and niguldipine did not stimulate the binding of $[^3H]$ vinblastine to p-gp in ADR5000 membranes. Niguldipine inhibited with an IC_{50} value of 171 ± 56 nM (maximum inhibition to $14\% \pm 13\%$ of control, $n = 3$), and $3\text{ }\mu\text{M}$ B9309-012 reduced $[^3H]$ vinblastine binding to 35% of control. The opposite effects of these compounds on $(-)-[^3H]BZDC\text{--}DHP$ and $[^3H]$ vinblastine labeling provide additional evidence that these radioligands label different sites on p-gp.

DISCUSSION

Considerable progress has been made recently to elucidate the structure of the p-gp. However, the molecular mechanism involved in the ATP-dependent translocation of its substrates from within either the membrane bilayer (Stein et al., 1994) or the cytoplasm (Gottesman & Pastan, 1993) to the extracellular side remains unclear. It is generally believed that binding of drugs to one or more binding domains on p-gp represents the initial step of transport. This is implied from the substrate specificity of p-gp and is evident from studies showing that p-gp substrates and chemosensitizers bind to p-gp. This was demonstrated mainly by photoaffinity labeling employing photoreactive derivatives of cytotoxics (Gottesman & Pastan, 1993) and chemosensitizers (Foxwell et al., 1989; Qian & Beck, 1990; Borchers et al., 1995; Safa et al., 1994). The concentration-dependent inhibition of $[^3H]$ azidopine photolabeling has widely been used as a biochemical assay to indirectly determine drug binding affinities for unlabeled drugs.

Although photolabeling experiments are suitable to identify p-gp active drugs these “binding assays” have clear disadvantages:

(1) The irreversible nature of photoaffinity labeling does not allow the determination of true binding inhibition constants (i.e., IC_{50} or K_i values).

(2) Covalent incorporation of photoligand occurs at low yield [below 20% of reversibly bound ligand for most aryl azides, Striessnig et al. (1986, 1987)]. Therefore higher ligand and receptor concentrations are usually employed to increase the amount of incorporated radioactivity. This facilitates detection of incorporated label (e.g., by reducing exposure times for fluorography) but results in higher apparent IC_{50} values as predicted by the law of mass action (Linden, 1982). Moreover, for many hydrophobic compounds, partitioning of free drug into hydrophobic compartments increases with protein concentration and may result in a reduction of apparent binding affinity (Boer et al., 1989).

(3) Inhibitors may be light-sensitive and chemically unstable under the conditions of photolabeling.

(4) Analysis of photoincorporated ligand is time consuming and requires detection of radioactivity after SDS–PAGE or immunoprecipitation.

Exact estimates for the affinity of drugs for p-gp can only be derived from reversible equilibrium binding experiments. Attempts to establish such techniques have been reported. K_d values of 300–38 300 nM were measured for several Ca^{2+} antagonists [$[^3H]$ devapamil, $[^3H]$ diltiazem (Cornwell et al., 1987), $[^3H]$ SR33557 (Jaffrezou et al., 1991)] and $[^3H]$ vinblastine (Cornwell et al., 1987). A detailed analysis of their binding properties was difficult due to the low affinities and/or unfavorable signal to noise ratios (Cornwell et al., 1987; Jaffrezou et al., 1991). The only exception is a recent report by Ferry and co-workers (1992), who described high-affinity ($K_D = 9$ nM) reversible labeling of a cytotoxic binding domain using $[^3H]$ vinblastine. $[^3H]$ Vinblastine dissociation kinetics were accelerated by DHPs. It was concluded that DHPs and cytotoxics label different sites on p-gp.

Using the novel DHP $(-)-[^3H]BZDC\text{--}DHP$, we report here the first reversible binding assay for a chemosensitizer. $(-)-[^3H]BZDC\text{--}DHP$ binding fulfills all criteria for the reversible labeling of a high-affinity chemosensitizer site on p-gp. Vinblastine-sensitive, protein concentration dependent binding was only detectable in membranes of resistant cells but not in the respective sensitive cell line. Comparable dissociation constants were derived from saturation analysis and kinetic studies. Reversible binding was inhibited by known p-gp active drugs. The relative potency of all chemosensitizers tested in this study correlated with their potency for the inhibition of rhodamine 123 accumulation.

Unlabeled vinblastine incompletely inhibited $(-)-[^3H]BZDC\text{--}DHP$ binding (and photolabeling). In contrast to BZDC–DHP itself, vinblastine’s inhibitory potency was significantly decreased by B9309-012. Both findings are incompatible with a simple competition of Vinca alkaloids with the site labeled by BZDC–DHP. Thus our data confirm the model by Ferry et al. (1992) proposing at least two distinct sites, for DHPs and the Vinca alkaloid cytotoxics, respectively. Our data extend and modify this model by demonstrating that DHPs interact with at least two distinct high-affinity chemosensitizer sites on p-gp (Figure 8). This is evident from the stereoselective modulation of $(-)-[^3H]BZDC\text{--}DHP$ binding by the niguldipine enantiomers. Dextran-guldipine biphasically inhibited radioligand binding, whereas niguldipine stimulated binding at submicromolar concentrations. This rules out niguldipine interaction with the $(-)-[^3H]BZDC\text{--}DHP$ -labeled site. Instead, niguldipine must interact with a distinct (or at least overlapping) site causing steric or allosteric stimulation of $(-)-[^3H]BZDC\text{--}DHP$

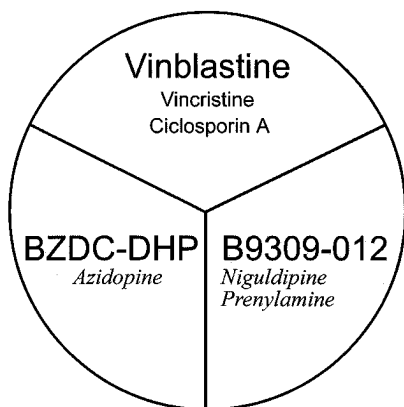


FIGURE 8: Proposed model of p-gp-associated drug receptor domains. Drugs that have not directly been shown to competitively interact with the respective binding domain are printed in italics.

binding in a ternary complex. Obviously, the substituted DHP ring does not confer selectivity for a single binding domain as it does on L-type Ca^{2+} channels (Glossmann & Striessnig, 1990). This argues against the existence of a DHP-selective binding domain on p-gp as proposed by Ferry et al. (1992). Instead, we postulate a model accounting for the existence of at least two chemosensitizer binding domains on p-gp (Figure 8): One is labeled by BZDC-DHP, and a second is labeled by the stimulatory B9309-012. Other stimulators, e.g., prenylamine and niguldipine, may also bind to the B9309-012 binding domain (Figure 8). Both chemosensitizer sites are (negatively) coupled to the vinblastine receptor domain via non-competitive mechanisms (vinblastine incompletely inhibits $(-)[^3\text{H}]\text{BZDC-DHP}$ binding, B9309-012 decreases vinblastine affinity). As shown in earlier studies (Ferry et al., 1992; Tamai & Safa, 1991) cyclosporin A also binds to the vinblastine receptor domain (Figure 8). It is tempting to speculate that the different receptor domains form overlapping parts of a larger area within p-gp that represents a "hot spot" for drug binding by providing a high density of suitable attachment points. Similarly, such a "hot spot" was detected for at least two structurally different classes of Ca^{2+} antagonists (dihydropyridines and benzothiazepines) on L-type Ca^{2+} channels near the extracellular opening of the ion pore (Watanabe et al., 1993; Hering et al., 1993; Prinz & Striessnig, 1993).

Taken together our experiments demonstrate that $(-)[^3\text{H}]\text{BZDC-DHP}$ is a novel specific tool for the irreversible and reversible labeling of a chemosensitizer binding domain on p-gp. It should be especially useful to study the effects of single p-gp mutations (Loo & Clarke, 1993; Kajiji et al., 1993; Safa et al., 1990) on the kinetics of BZDC-DHP binding and on its interaction with the noncompetitively coupled receptor domains. Combined with the analysis of functional effects this will allow more detailed insight into the molecular pharmacology of human p-gp.

ACKNOWLEDGMENT

We thank Dr. V. Gekeler and Dr. W. Ise (Byk-Gulden, Konstanz, Germany) for providing CCRF-ADR5000 membranes and Ms. E. Penz, S. Haas, and A. Schödl for excellent technical assistance. We are grateful to Dr. D. Ahern (Dupont New England Nuclear) for preparation of the tritium-labeled BZDC-NHS and Prof. M. Przybylski (Fakultät für Chemie, Universität Konstanz, Germany) for continuous support.

REFERENCES

- Boer, R., Grassegger, A., Schudt, C., & Glossmann, H. (1989) *Eur. J. Pharmacol.* 172, 131.
- Boer, R., Haas, S., & Schödl, A. (1994) *Eur. J. Cancer* 30A, 1117.
- Borchers, C., Ulrich, W.-R., Klemm, K., Ise, W., Gekeler, V., Haas, S., Schödl, A., Conrad, J., Przybylski, M., & Boer, R. (1995) *Mol. Pharmacol.* 48, 21.
- Cornwell, M. M., Gottesmann, M. M., & Pastan, I. H. (1986) *J. Biol. Chem.* 261, 7921.
- Cornwell, M. M., Pastan, I., & Gottesmann, M. M. (1987) *J. Biol. Chem.* 262, 2166.
- DeLean, A., Munson, P. J., & Rodbard, D. (1978) *Am. J. Physiol.* 4, E97.
- Ferry, D. R., Rombusch, M., Goll, A., & Glossmann, H. (1984) *FEBS Lett.* 169, 112.
- Ferry, D. R., Russell, M. A., & Cullen, M. H. (1992) *Biochem. Biophys. Res. Commun.* 188, 440.
- Fleming, G. F., Amato, J. M., Agresti, M., & Safa, A. R. (1992) *Cancer Chemother. Pharmacol.* 29, 445.
- Ford, J., & Hait, W. N. (1990) *Pharmacol. Rev.* 42, 155.
- Foxwell, B. M. J., Mackie, A., Ling, V., & Ryffel, B. (1989) *Mol. Pharmacol.* 36, 543.
- Friche, E., Demant, E. J. F., Sehested, M., & Nissen, N. I. (1993) *Br. J. Cancer* 67, 226.
- Glossmann, H., & Striessnig, J. (1990) *Rev. Physiol. Biochem. Pharmacol.* 114, 1.
- Gottesman, M. M., & Pastan, I. (1993) *Annu. Rev. Biochem.* 62, 385.
- Hait, W. N., Gesmonde, J. F., Murren, J. R., Yang, J., Chen, H., & Reiss, M. (1993) *Biochem. Pharmacol.* 45, 401.
- Hering, S., Savchenko, A., Strübing, C., Lakitsch, M., & Striessnig, J. (1993) *Mol. Pharmacol.* 43, 820.
- Hofmann, J., Wolf, A., Spitaler, M., Böck, G., Drach, J., Ludescher, C., & Grunicke, H. (1992) *J. Cancer Res. Clin. Oncol.* 118, 361.
- Horton, J. K., Thimmaiah, K. N., Harwood, F. C., Kuttess, J. F., & Houghton, P. J. (1993) *Mol. Pharmacol.* 44, 552.
- Hyafil, F., Vergely, C., Du Vignaud, P., & Grand-Perret, T. (1993) *Cancer Res.* 53, 4595.
- Jaffrezou, J.-P., Herbert, J.-M., Levade, T., Gau, M.-N., Chatelain, P., & Laurent, G. (1991) *J. Biol. Chem.* 266, 19858.
- Kajiji, S., Talbot, F., Grizzuti, K., Van Dyke-Phillips, V., Agresti, M., Safa, A. R., & Gros, P. (1993) *Biochemistry* 32, 4185.
- Kamiwatari, M., Nagata, Y., Kikuchi, H., Yoshimura, A., Sumizawa, T., Shudo, N., Salpda, R., Seto, K., & Akiyama, S. (1989) *Cancer Res.* 49, 3190.
- Keller, R. P., Altermatt, H. J., Nooter, K., Poschmann, G., Laissue, J. A., Bollinger, P., & Hiestand, P. C. (1992) *Int. J. Cancer* 50, 593.
- Knaus, H. G., Striessnig, J., Hering, S., Marrer, S., Schwenner, E., Hölte, H.-D., & Glossmann, H. (1992) *Mol. Pharmacol.* 41, 298.
- Linden, J. (1982) *J. Cyclic Nucleotide Res.* 8, 163.
- Loo, T. W., & Clarke, D. M. (1993) *J. Biol. Chem.* 268, 19965.
- Lowry, O. H., Rosebrough, N. H., Farr, A. L., & Randall, F. J. (1951) *J. Biol. Chem.* 193, 265.
- Moebius, F. F., Burrows, G. G., Striessnig, J., & Glossmann, H. (1993) *Mol. Pharmacol.* 43, 139.
- Moebius, F. F., Hanner, M., Knaus, H. G., Weber, F., Striessnig, J., & Glossmann, H. (1994) *J. Biol. Chem.* 269, 29314.
- Mourey, R. J., Estevez, V. A., Marecek, J. F., Barrow, R. K., Prestwich, G. D., & Snyder, S. H. (1993) *Biochemistry* 32, 1719.
- Olszewski, I. D., Dorman, G., Elliott, J. T., Hong, Y., Ahern, D. G., & Prestwich, G. D. (1995) *Bioconjugate Chem.* 6, 395.
- Pastan, I., & Gottesman, M. M. (1991) *Annu. Rev. Med.* 42, 277.
- Prinz, H., & Striessnig, J. (1993) *J. Biol. Chem.* 268, 18580.
- Qian, X., & Beck, W. T. (1990) *Cancer Res.* 50, 1132.
- Reymann, A., Looft, G., Woermann, C., Dietel, M., & Erttmann, R. (1993) *Cancer Chemother. Pharmacol.* 32, 25.
- Safa, A. R., Glover, C. J., Sewell, J. L., Meyers, M. B., Biedler, J. L., & Felsted, R. L. (1987) *J. Biol. Chem.* 262, 7884.
- Safa, A. R., Stern, R. K., Choi, K., Agresti, M., Tamai, I., Mehta, N. D., & Roninson, I. B. (1990) *Proc. Natl. Acad. Sci. U.S.A.* 87, 7225.

- Safa, A. R., Agresti, M., Bryk, D., & Tamai, I. (1994) *Biochemistry* 33, 256.
- Stein, W. D., Cardarelli, C., Pastan, I., & Gottesmann, M. M. (1994) *Mol. Pharmacol.* 45, 763.
- Striessnig, J., Moosburger, K., Goll, A., Ferry, D. R., & Glossmann, H. (1986) *Eur. J. Biochem.* 161, 603.
- Striessnig, J., Knaus, H. G., Grabner, M., Moosburger, K., Seitz, W., Lietz, H., & Glossmann, H. (1987) *FEBS Lett.* 212, 247.
- Tamai, I., & Safa, A. R. (1991) *J. Biol. Chem.* 266, 16796.
- Watanabe, T., Kalasz, H., Yabana, H., Kuniyasu, A., Mershon, J., Itagaki, K., Vaghy, P. L., Naito, K., Nakayama, H., & Schwartz, A. (1993) *FEBS Lett.* 334, 261.
- Yoshimura, A., Kuwazuru, Y., Sumizawa, T., Ichikawa, M., Ikeda, S.-I., Uda, T., & Akiyama, S.-I. (1989) *J. Biol. Chem.* 264, 16282.

BI951912U